ACS OMEGA

Open Access

http://pubs.acs.org/journal/acsodf

Review

A Practical Toolkit for the Detection, Isolation, Quantification, and Characterization of Siderophores and Metallophores in Microorganisms

Ana F. R. Gomes, Emília Sousa,* and Diana I. S. P. Resende*

Cite This: *ACS Omega* 2024, 9, 26863−26877

Read Online

ACCESS | Metrics & More | Article Recommendations

ABSTRACT: Siderophores are well-recognized low-molecular-weight compounds produced by numerous microorganisms to acquire iron from the surrounding environments. These secondary metabolites can form complexes with other metals besides iron, forming soluble metallophores; because of that, they are widely investigated in either the medicinal or environmental field. One of the bottlenecks of siderophore research is related to the identification of new siderophores from microbial sources. Herein we have compiled a comprehensive range of standard and updated methodologies that have been developed over the past few years to provide a comprehensive toolbox in this area to current researchers.

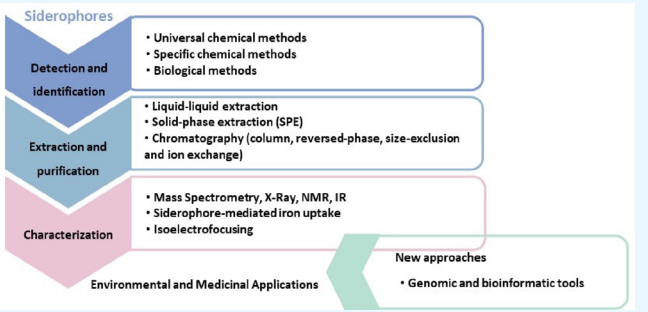

1. INTRODUCTION

Siderophores are low-molecular-weight iron-chelating agents produced by living organisms such as bacteria, yeasts, fungi, and plants.[1] While growing under low-iron conditions, microorganisms secrete these high-affinity iron-chelating molecules to scavenge and solubilize iron from the extracellular environment, safeguarding the supply of this important metal that is essential for their growth, replication, and metabolism.[2] In the environment, most of the iron is found in the form of insoluble ferric oxide/hydroxide complexes due to the fast oxidation of Fe^{2+} to Fe^{3+}, and siderophores have a high affinity for iron's ferric form (Fe^{3+}). The siderophore−iron complex is recognized by high-affinity receptor proteins on the outer membrane of the bacteria and internalized by active transport. Iron is then released from siderophores, typically via the reduction of Fe^{3+} to Fe^{2+} by microbe-mediated redox processes.[3]

Over 500 siderophores have been identified and classified into three primary groups based on the type of ligands that iron binds: catecholates, hydroxamates, and α-hydroxy carboxylates (Figure 1).[4,5] Nevertheless, these known siderophores represent only a fraction of the siderophores produced endogenously by bacteria, yeasts, fungi, and plants. Examples of siderophores include mixed-type siderophores, such as pyoverdine (Figure 6), staphyloferrin A, fimsbactin C, pyochelin, and yersiniabactin, which contain more than one functional group;[6−8] catecholates such as enterobactin, bacillibactin, and salmochelin S4 (Figure 2); hydroxamates such as desferrioxamine B, rhodotorulic acid, coprogen, ferrichrome, and *N*,*N*′,*N*″-triacetylfusarinine C (Figure 4); and α-hydroxy carboxylates such as rhizoferrin and staphylopherrin A (Figure 7).

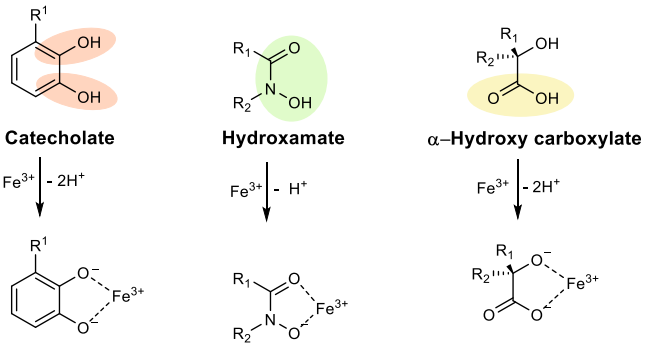

Figure 1. Classification of siderophores according to the chemical nature of their binding site.

Siderophores show great potential for medical use due to their ability to bind to metals and are commonly employed in clinical settings for managing iron overload illnesses stemming

Received: March 29, 2024
Revised: May 29, 2024
Accepted: May 30, 2024
Published: June 11, 2024

from frequent blood transfusions.[1,9] Additionally, the manipulation of the microbial iron transport pathways to deliver antimicrobials to the cell using siderophores has been explored as a potential strategy to overcome antimicrobial resistance.[10] This approach, often referred to as the "Trojan horse" approach, involves utilizing siderophores as a means of transporting antimicrobials into the cell.[11,12] Hence, the conjugation of iron-chelating microbial siderophores to antimicrobial agents can be used to enhance uptake and antimicrobial potency.[13] Siderophores can bind other metal ions besides iron, and usually the most effective are those that have three bidentate ligands per molecule, forming a hexadentate complex.[14] Hexadentate siderophores exhibit a high affinity for Fe^{3+} and its mimetic Ga^{3+}, which can compete with Fe^{3+} in many binding interactions due to its similar atomic radius (Ga^{3+} = 0.62 Å vs. Fe^{3+} = 0.65 Å)[15] and valence. In cases where iron is replaced by radionuclides such as gallium-68, a positron emitter with a short half-life (68 min) capable of forming highly stable complexes with the siderophores, targeting imaging of infections by positron emission tomography (PET) is possible.[16,17] Other medical applications are reported in the field of malaria and cancer, wound healing, or even for biosensors.[1,9,12]

Apart from iron and gallium, siderophores can chelate with several other metals, forming soluble metallophores with divalent cations such as Zn^{2+}, Ni^{2+}, Cd^{2+}, Cu^{2+}, and Pb^{2+} and trivalent cations including Al^{3+}, In^{3+}, Mn^{3+}, V^{3+}, and Co^{3+}. Additionally, they can also form complexes with actinides like Th^{4+}, U^{4+}, and Pu^{4+}[18] and lanthanides.[19] This capacity makes them promising candidates for the bioremediation of ecosystems, as they can remove heavy metals from contaminated areas, weathering soil minerals and enhancing plant growth, and improve the contaminant degradation abilities of microbes, or they can be used as biocontrol agents[1,8,20,21] for remediation purposes, as they can mobilize diverse metals and efficiently remove them from contaminated ecosystems.

All the previously described siderophore applications have been widely reviewed over the years,[5,9,10,17,20−22] highlighting their numerous applications in either the medical or environment field, with most of the authors concluding that there is still a long and promising way to go, with many opportunities to further use the available knowledge toward the development of new and improved approaches in both fields. The characterization of new siderophores can further spark the synthesis of improved siderophore mimetics, which can potentially lead to the implementation of new strategies. Nevertheless, the current literature lacks an updated practical toolkit for detecting, isolating, and characterizing siderophores and metallophores. The existing protocols are either outdated[23−25] or limited[26,27] and do not encompass the full range of methodologies available. This highlights the need for more comprehensive and up-to-date protocols in this area. Gathering a comprehensive range of standard and improved methodologies that have been developed over the last years, this review aims to assist researchers in the identification of new siderophores from microbial sources.

2. DETECTION AND IDENTIFICATION OF SIDEROPHORES IN MICROBIAL CULTURES

Numerous techniques have been devised to universally identify various types of siderophores by leveraging their biological and functional characteristics.[24] The majority of the functional assays are based on the chrome azurol S (CAS) universal assay. This assay uses a growth medium containing both essential nutrients and inhibitory compounds, making it unsuitable to cultivate certain microorganisms like fungi and Gram-positive bacteria.[28] A number of modifications to the CAS assay have been introduced, including the CAS agar plate technique. Early modifications were found to be time-consuming and ineffective, as they could only identify one type of microorganism at a time. However, recent methodologies use fewer toxic surfactants and yield comparable results while allowing the growth of yeast and fungi. Although widely employed, the CAS assay is limited by its nonspecificity. Other colorimetric- and fluorescence-based methods are more specific for different types of siderophores, allowing the identification of their class. These alternative methods can be used in conjunction with CAS detection to indicate the specific type of siderophores produced, such as catecholates, hydroxamates, or carboxylates.

2.1. Universal Chemical Methods for Siderophore Detection. The CAS assay, a frequently used universal colorimetric assay developed by Schwyn and Neiland, is one of the most widely used screening methods for detecting siderophores.[29] This assay involves a competition between the siderophore and the ferric complex of the CAS dye for iron. Due to a higher affinity for iron by the siderophore, the metal is removed from the dye by the siderophore. Consequently, the dye changes its color from blue to orange, indicating that the siderophore strongly chelates the iron from the iron−dye complex, and the dye becomes free in the medium.[30] One disadvantage of this methodology lies in the presence of hexadecyltrimethylammonium bromide (HDTMA) in the medium,[29] a detergent component that is highly toxic for some microorganisms such as Gram-positive bacteria and fungi, inhibiting the growth of both when present in high concentrations.[31] To solve this problem, several modifications of the CAS universal assay were performed over the years. One modification involves the addition of an adsorbent resin, XAD-4 adsorbent polystyrene, to the CAS-malt extract blue agar plates to neutralize the excess HDTMA.[31] This modification has proven effective in enabling the growth of 10 hymenomycetous (fungi) isolates, with the CAS assay revealing that all of them were positive for siderophore production.[31] The incorporation of the CAS-blue dye in a medium with no contact with the microorganisms tested constitutes another methodology to enable the use of the CAS blue agar medium to a broader range of Gram-positive bacteria and fungi while circumventing the issues caused by the toxicity of the HDTMA detergent.[32] The dye can either be applied as a solution test or incorporated into the solid growth medium for direct plating mode, both for the screening of several microorganism siderophore producers.[30] Petri dishes can be used to test several strains of fungi (basidiomycetes, deuteromycetes, ascomycetes, and zygomycetes) and bacteria (Gram-positive and -negative) by splitting the surface using half for the cultivation medium and half for the CAS detection medium. Although this methodology allows for the development of a wide variety of microorganisms, it has been revealed to be extremely laborious and time-consuming, since it only permits the identification of one single type of microorganism per plate.[32] The use of an overlay technique, in which a modified CAS medium is cast upon culture agar plates (overlaid CAS, O-CAS), allows previous methodological limitations to be surpassed, avoiding the above-mentioned problems of toxicity and growth inhibition while allowing the

https://doi.org/10.1021/acsomega.4c03042
ACS Omega 2024, 9, 26863−26877

Table 1. Advantages and Disadvantages of the Different Modifications to the CAS Assay

assay[ref(s)]	methodology	advantages (↑)/disadvantages (↓)
CAS[29]	Siderophores scavenge iron from an Fe−CAS−hexadecyltrimethylammonium bromide complex; release of the CAS dye results in a color change from blue to orange.	↑ simple methodology ↓ presence of HDTMA in the medium, which is highly toxic for some microorganisms, inhibiting their growth
CAS modification[31]	Addition of an adsorbent resin, XAD-4 adsorbent polystyrene, to neutralize the excess HDTMA.	↑ effective in enabling the growth of 10 hymenomycetous (fungi) isolates
CAS modification[32]	The dye can either be applied as a solution test or incorporated into the solid growth medium for direct plating mode, both for the screening of several microorganism siderophore producers.	↑ wide variety of microorganisms ↓ extremely laborious and time-consuming
O-CAS[28]	Use of an overlay technique: a modified CAS medium is cast upon culture agar plates.	↑ identification of more than one siderophore-producing strain at once ↑ results available in less than half an hour ↑ suitable for any kind of microorganism and growth medium ↑ neither the reagents nor the pH causes inhibition of growth ↑ possible to recover the microorganisms from the original culture medium and reuse them, avoiding replicas
SD-CASA[34]	Performed on both the microorganism culture supernatant as an inducer and the microorganisms themselves as main producers.	↑ quantitative and low-cost methodology
CAS modification[33]	Replacement of HDTMA by DDAPS as the surfactant	↑ less toxic to the microorganism while producing similar results
high-throughput CAS shuttle assay[35,36]	Use of a 96-well microplate with CAS reagent. • 96-channel manual pipetting workstation[36] • MM9 growth medium replaced by a diluted growth medium in the absence of artificial iron depletion[35]	↑ fast identification ↑ mimic the low concentrations of organic compounds in the natural environment
CAS modification[37]	Use of azo dyes (MO and EBT) to replace the common CAS dye.	↑ lower costs
CAS modification[38,39]	Monitor chelation of elements other than Fe^{2+}, including Mn^{2+}, Co^{2+}, Ni^{2+}, Cu^{2+}, Zn^{2+}, Mg^{2+}, V^{3+}, Se^{4+}, and Te^{2+}.	↑ evaluation of siderophore production with cations other than iron

detection of a variety of siderophore-producing microorganisms at once.[28] These methodologies have been redesigned and optimized to enable the simultaneous identification of multiple siderophore-producing strains in less than 30 min. They are applicable to all types of microorganisms and growth media and tailored specifically for siderophore-producing microorganisms, as evidenced by the lack of medium color change in many strains during the selection process. Additionally, neither the reagents nor the pH levels hinder the growth of microorganisms.[28] In addition, it is possible to recover fungi from the original culture medium and reuse them, avoiding the use of replicas.[28] The replacement of HDTMA by *N*-dodecyl-*N*,*N*′-dimethyl-3-amino-1-propanesulfonate (DDAPS) as the surfactant in the CAS assay is also a promising strategy to optimize the development of siderophore-producing fungi since DDAPS is less toxic to the microorganism and produces similar results[33]

The simple double-layered CAS agar (SD-CASA) assay was developed as a quantitative, low-cost methodology to screen potential biocontrol microorganisms based on their siderophore production.[34] This modified CAS assay involved the use of paper-disc agar diffusion to inoculate a specific amount of bacteria suspension onto CAS agar plates.[34] The authors used this methodology to assess the impact of pH, carbon−nitrogen ratio, and type of exogenous amino acids of the medium on siderophore production by *Bacillus subtilis* QM3 and growth of the referred strain.[34]

Although the CAS assay relies on agar plate cultivation and uses the CAS reagent under iron-depleted conditions by using a modified M9 (MM9) medium devoid of iron, the MM9 medium is not always ideal for the growth of a diverse range of microorganisms. Commonly used growth media are also not suitable for the CAS assay because of their high iron and nutrient content. A recent study explored a high-throughput CAS shuttle assay in a 96-well microplate in which a concentrated CAS reagent was used and the MM9 growth medium was replaced by a diluted growth medium in the absence of artificial iron depletion.[35] The use of the diluted growth medium in the CAS assay was intended to mimic the low concentrations of organic compounds in the natural environment.[35] High-throughput detection of siderophore production can also be achieved by combining the CAS assay with a 96-channel manual pipetting workstation.[36] In a modified CAS assay method, siderophore production was assayed in 2150 representative bacterial members.[36] Besides all the above-mentioned modifications to the CAS assay, the possibility of using azo dyes [methyl orange (MO) and Eriochrome black T (EBT)] to replace the common CAS dye (more expensive) revealed that EBT dye, in controlled concentrations (20−30 ppm), allows siderophore detection through a different color change (from red to blue).[37] Even though iron is the metal of choice for the referred methods, the production of siderophores can also be evaluated with different cations (Mn^{2+}, Co^{2+}, Ni^{2+}, Cu^{2+}, and Zn^{2+} according to ref 38 and Mg^{2+}, V^{3+}, Mn^{2+}, Co^{2+}, Ni^{2+}, Cu^{2+}, Zn^{2+}, Se^{4+}, and Te^{2+} according to ref 39) by CAS; supplemented agar plate shows that use of iron is not required in this type of assay to detect siderophores since the competition for iron or any of the other tested metals is similar. Despite the proven utility of the CAS assay (Table 1), including all the valuable modifications performed throughout the years, it is essential to emphasize that this methodology presents a noteworthy drawback: any substance secreted by the microorganism that is capable of forming a complex with iron or another metal but is not a siderophore will also be detected in this type of test.

https://doi.org/10.1021/acsomega.4c03042
ACS Omega 2024, 9, 26863−26877

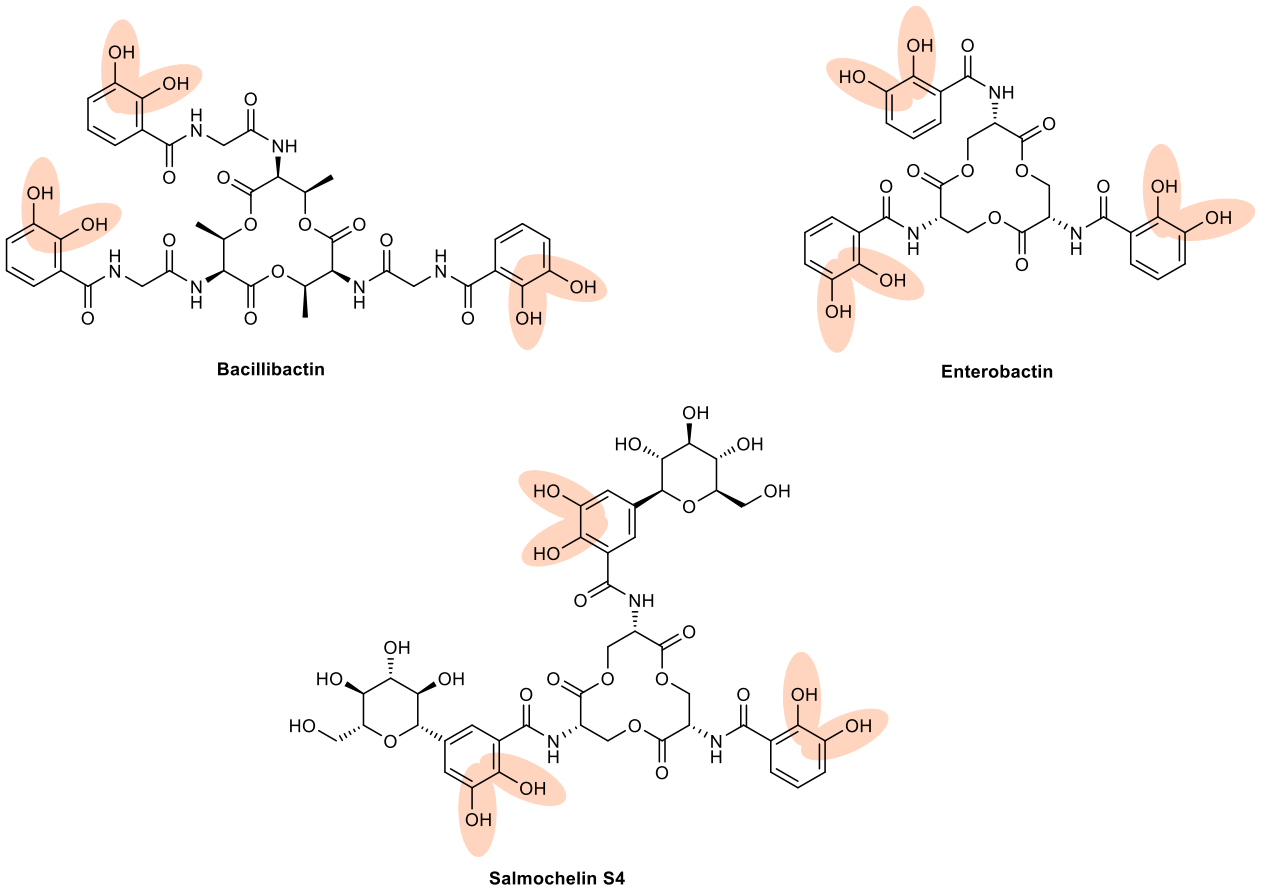

Figure 2. Representative structures of catecholate-type siderophores.

The quantification of siderophores produced by microorganisms can be achieved through spectrophotometric estimation. In this traditional method, CAS reagent is mixed with microbial culture supernatant, and the amount of siderophore is estimated by a colorimetric/spectrophotometric method, measuring the absorbance of each sample individually. This quantification is usually performed by extrapolating a standard curve using a CAS assay solution. The CAS solution is mixed with the culture supernatant, and the absorbance of the final solution is measured at 630 nm after incubation (1−2 h). The siderophore content is then calculated according to the equation

$$\%\ \text{siderophore units} = \frac{A_r - A_s}{A_r} \times 100$$

where A_r is the reference absorbance and A_s is the absorbance of the sample.[25,40] This methodology was used throughout the years, with small modifications to the CAS assay. A CAS agar diffusion (CASAD) assay, a modification of the universal plate and liquid CAS assay, can be used to quantitatively measure total siderophores existing in any biological fluids.[41] This improved protocol takes advantage of the universal CAS assay, where the iron bound to CAS is easily chelated by siderophores to produce a color change from blue to orange, and simultaneously takes advantage of the principle of antimicrobial diffusion, where the siderophores applied to the hole diffuse to radially build a concentration gradient from the center.[42] Another methodology suitable for the quantification of siderophores produced in solid media consist in measuring the rate of color change of CAS medium (mm/day) with the production in liquid medium, evaluated as % siderophore units.[43] This methodology was applied to three species of *Aspergillus* that were cultivated in the absence or presence of iron; a similar profile regarding siderophore production was observed on both media.[43] However, these methodologies require large amounts of chemicals, time, labor, and space. For this reason, a modified microplate method for siderophore quantification was developed.[30] Specifically, the absorbance is read using a microplate reader in a 96-well microplate at 630 nm, and siderophores are quantitated using the equation shown above. This method was shown to be less laborious, cheaper, and less toxic for the environment (less amount of CAS reagent used).[30] Additionally, it can be used for quantification of siderophores by any bacteria as a better alternative to the routine colorimetric method. The universal CAS assay originally designed for bacterial siderophore detection and later designed for fungus was recently adapted for the diffusive equilibrium in thin-film gel technique (DET).[44] Hence, the CAS-DET device matches the colorimetric reagent CAS with DET. This improved methodology allows the detection of all the ligands with higher affinity for iron than the CAS ligand, proving to be ideal for mapping the siderophores in an artificial environment such as agar medium, and, combined with the use of the hyperspectral imaging, to quantify them at micromolar scale.[44] Additionally, it allows detection of the production of siderophores in the rhizosphere and their quantification at a micromolar level.[44]

2.2. Specific Chemical Methods for Siderophore Type Identification. *2.2.1. Identification of Catecholate-Type Siderophores. Arnow Colorimetric Test.* The Arnow colori-

https://doi.org/10.1021/acsomega.4c03042
ACS Omega 2024, 9, 26863−26877

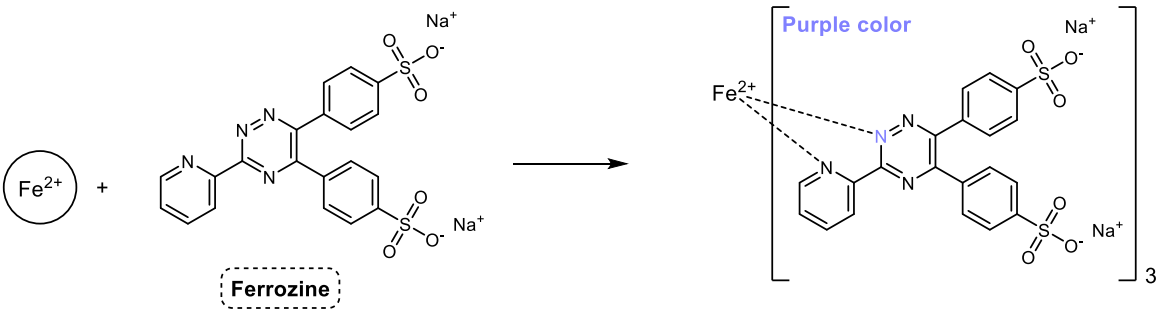

Figure 3. Principle of the method to evaluate Fe^{2+} chelating activity using ferrozine.[50]

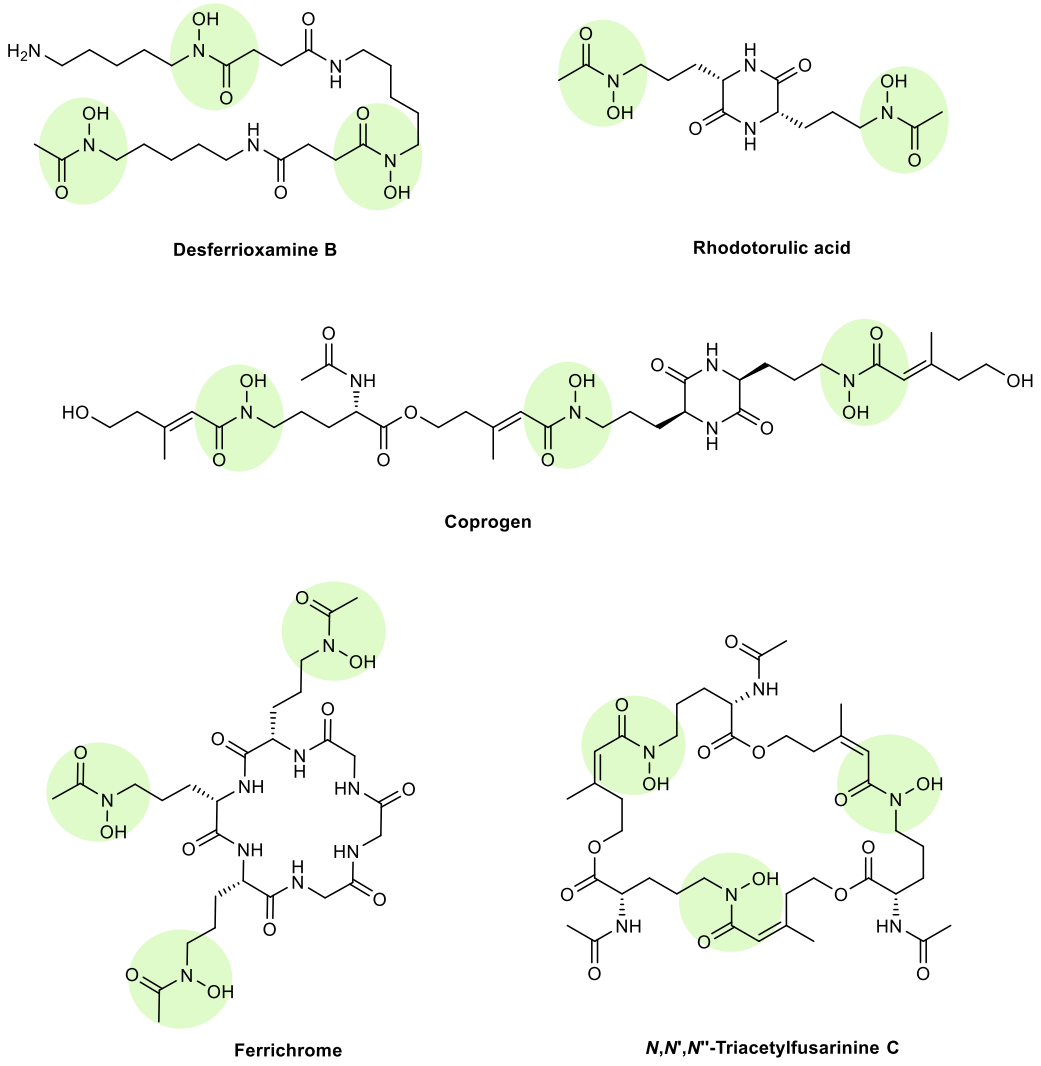

Figure 4. Representative structures of hydroxamate-type siderophores.

metric test, developed by Arnow in 1937,[45] is commonly used for identifying catecholate-type siderophores. This test detects the presence of these siderophores by the yellow color formation when the catechol group combines with nitrous acid (HNO_2).[25] Compounds containing phenolic hydroxy groups yield colored compounds when heated with sodium nitrite. It was hypothesized that hydrogen ions from the phenolic hydroxy groups combine with nitrite ions (NO_2^-), and the molecular nitrous acid then forms NO compounds with the phenols. If sodium nitrite is added to an acid solution, the nitrous acid that is formed decomposes fairly rapidly. Sodium molybdate is therefore added to prevent rapid decomposition.[45] Under alkaline conditions, the color can turn into a deep-red shade, and the intensity of the color relies on the amount of catechol present.[25] Similarly, the presence of the 2,3-dihydroxybenzoyl fragment, which represents the catechol moiety, can be confirmed by analyzing the UV spectrum since it presents three absorption bands (320 nm, 250 nm, and the most intense at 210 nm).[23,46] For instance, *B. subtilis* strain LSBS2 produces a siderophore that has been identified as bacillibactin after testing positive in the Arnow assay (Figure 2).[47] In some cases, both the Csaky test

https://doi.org/10.1021/acsomega.4c03042
ACS Omega 2024, 9, 26863−26877

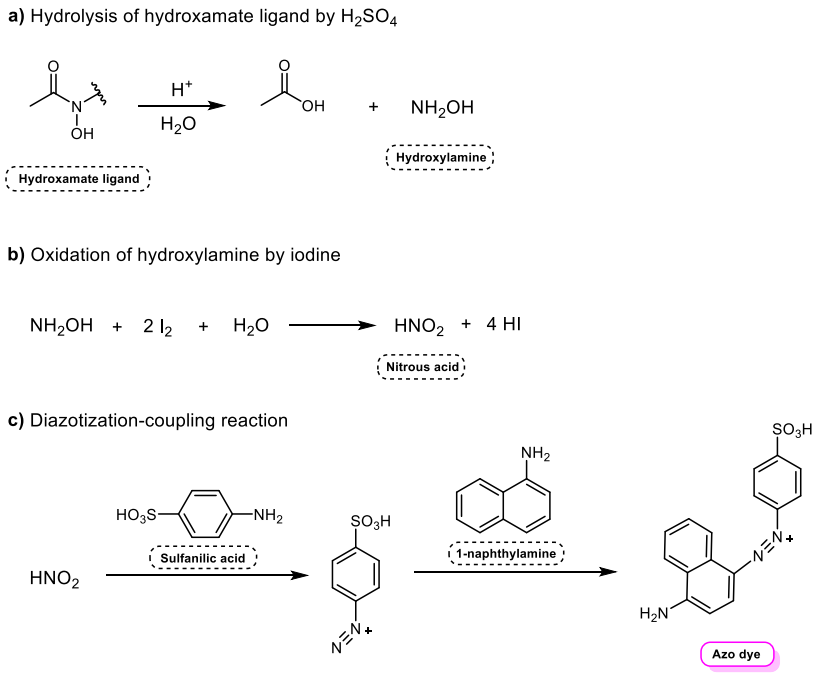

Figure 5. Csaky test reactions: (a) hydrolysis of hydroxamate ligand by sulfuric acid to originate the hydroxylamine; (b) oxidation of hydroxylamine by iodine solution to originate nitrous acid; (c) diazotization reaction with the formation of the diazonium cation that will couple with 1-naphthylamine (coupling agent) to obtain a colored dye (deep-pink color).[51]

(mentioned below) and Arnow test show positive results, as seen in *Azotobacter vinelandii* Deutsche Sammlung von Mikroorganismen and Zellkulturen (DSM) 2289 when testing for the presence of catechol and hydroxamate moieties.[48] This suggests that the siderophores produced by *A. vinelandii* may be of the mixed type or that the bacteria can produce two different types of siderophores.[48] The ferric chloride ($FeCl_3$) test (see below) can also detect both the catecholate-type and hydroxamate-type siderophores by producing a wine color or an orange color, respectively.[49]

$FeCl_3$ Test. The $FeCl_3$ test is also mentioned as a colorimetry-based method (Figure 3), whose foundation is the formation of a complex between the Fe^{2+} ion and the reagent 3-(2-pyridyl)-5,6-bis(4-phenylsulfonic acid)-1,2,4-triazine (ferrozine) (Figure 3). The complex has a purple color, and its absorbance can be measured at a wavelength of 562 nm. The chelating potential is evaluated by the decrease in absorbance at the referred wavelength. Thus, the lower the absorbance, the higher the chelating potential.[50]

2.2.2. Identification of Hydroxamate-Type Siderophores. Csaky Test. The Csaky test (developed by Csaky in 1948 as a modification of the Blom method that involved a direct determination of hydroxylamine) is specific to determine hydroxamate-type siderophores (Figure 4) and is based on the chemical characteristics of these siderophores.[25,51] This assay depends on the formation of NO_2^- via the oxidation of hydroxylamine (NH_2OH) by an iodine solution and the formation of a colored dye by coupling to 1-naphthylamine.[48] Initially, sulfuric acid (H_2SO_4) is added to hydrolyze the hydroxamate ligand following oxidation by the iodine (Figure 5). This hydrolysis is necessary since oxidation by iodine does not occur directly on secondary hydroxamic acids.[51] After oxidation, the HNO_2 is diazotized and coupled with the respective coupling agent, sulfanilic acid.[51] The presence of a deep-pink color indicates the presence of the hydroxamate-type siderophore.[25] Purified desferrioxamine can be used as a standard, showing a red color upon reaction with the azo dye.[25]

Ferric Perchlorate Assay. The ferric perchlorate assay (developed by Atkin in 1970) also identifies hydroxamate-type siderophores and is represented by the appearance of an orange-red or purple color.[24,52] Since this is a test for hydroxamic acids, which form di-, tetra-, and hexadentate derivates with Fe^{3+} ion, the absorbance covers a range from 300 to 500 nm.[53] In particular, at low pH in perchloric acid ($HClO_4$), this assay can also detect other siderophores that can form stable complexes with iron.[24]

Tetrazolium Test. The tetrazolium test is a simple way to detect hydroxamates. By adding a few drops of NaOH and the corresponding sample to the tetrazolium salt, the presence of an hydroxamate siderophore can be confirmed by the emergence of a deep-red color.[54] This test is based on the hydrolysis of hydroxamate groups, which reduces the tetrazolium salt, as reported by Kotasthane et al.[55] Of the three assays presented for the identification of hydroxamate-type siderophores, the Csaky assay is considered to be the most sensitive.[51]

2.2.3. Identification of Carboxylate-Type Siderophores. Vogel Chemical Test. Carboxylate-type siderophores can be determined using Vogel's chemical test and Shenker's spectrophotometric test.[2] In the Vogel assay, phenolphthalein is added to a solution of NaOH. Sterile deionized water is then added to the mixture until the appearance of a light-pink color. Disappearance of color by the addition of culture supernatant indicates the presence of siderophores with a carboxylate nature. The latter is specifically used to identify hydroxycarboxylate-type siderophores. To do so, full wavelength scanning is conducted to identify the presence of a hydroxycarboxylate copper−siderophore complex. If the

https://doi.org/10.1021/acsomega.4c03042
ACS Omega 2024, 9, 26863−26877

solution contains hydroxycarboxylate-type siderophore, the maximum absorption peak is between 190 and 280 nm.[56]

2.2.4. Identification of Pyoverdines. Fluorescent siderophores (e.g., pyoverdines; Figure 6) can be detected by a

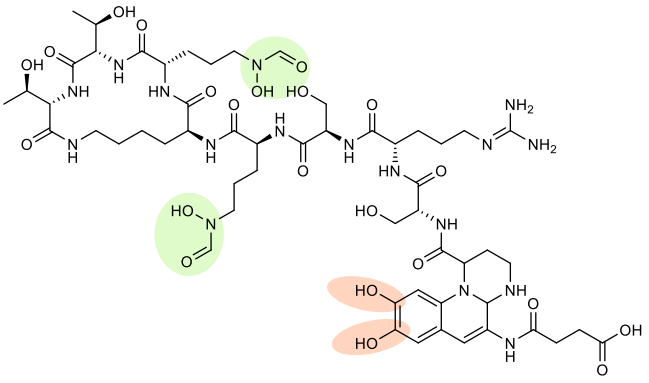

Figure 6. Structure of pyoverdine.

fluorescence-based method. These types of siderophores have an intrinsic fluorescence, and upon binding to metal ions, the fluorescence is quenched.[57] Pyoverdine contains a chromophore, the quinoline derivative 2,3-diamino-6,7-dihydroxyquinoline, that confers both color and fluorescence, and an acyl chain is attached to the NH_2 group of the chromophore with a peptide chain linked by its N-terminus to the carboxyl group of the chromophore.[58] Fluorescence quenching can be evaluated by adding different metals to metal-free culture filtrates and incubating them for a specific period before measurement. To accurately estimate the total amount of siderophores produced by the organism, it is essential to know the fluorescence quenching of siderophores.[25] The fluorescence of pyoverdine can be observed at an excitation wavelength of 345 nm and an emission wavelength of 460 nm. A study was conducted to investigate the correlation between the concentration of pyoverdine and the fluorescence intensity at 460 nm in a diluted growth medium. The fluorescence intensity of pyoverdine was measured using a 96-well microplate reader, and the calibration curves generated were used to estimate the amount of pyoverdine in the supernatant of each sample culture.[35]

Since the 1980s, about 50 structurally different pyoverdines have been described, each with a specific peptide chain varying by the aminoacyl residue type and number. Rapid methods of pyoverdine differentiation have been developed to overcome redundancies among structural studies.[59] The two most practical methods are isoelectrophoresis analysis of the pyoverdine content of iron-starved bacterial culture supernatants (pyoverdine typing by isoelectric focusing, PVD-IEF) and bacterial specificity determination of pyoverdine-mediated iron uptake. These methods have allowed the recognition of numerous original compounds representing most of the 50 structurally defined pyoverdines and about 60 additional compounds with unknown structures.[59] However, some pyoverdines cannot be distinguished because of identical IEF and iron uptake behaviors due to small structural differences. These discrete changes do not affect the overall charges of the molecules and do not affect their IEF patterns[59]

2.3. Biological Methods for Siderophore Detection. Bioassays involving a tester strain are a reliable method for identifying various types of siderophores. For instance, *Escherichia coli* was used to estimate the presence of ferrichrome siderophores (Figure 7) in soil-water samples.[24,60] Ferrichrome is capable of stimulating the growth of *E. coli* under iron-deprived conditions by competing with ethylenediamine-*N*,*N*′-bis(2-hydroxyphenylacetic acid) (EDDHA), an iron chelator, which is added to the medium to inhibit the growth of the tester strain.[61]

Another example was developed to detect siderophores (containing monoprotic keto−hydroxy bidentate ligands) from low-iron cultures using bacteria from the Proteeae group.[62] *Morganella morganii* SBK3 was chosen as an indicator strain, and the assay involved testing siderophore-containing disks on agar with a ferrous iron chelator. Growth inhibition reversal indicated siderophore presence, and various siderophores, including α-hydroxycarboxylates and others, showed significant growth stimulation.[62] A few other examples were reported;[63−66] however, the CAS assay rapidly surpassed this methodology due to its simplicity and instant results.

3. SIDEROPHORE EXTRACTION AND PURIFICATION

The direct assessment of the concentration of natural siderophores in the environment can be challenging due to the high complexity of sample matrices (soil extracts, pore water, seawater, and microbial culture media).[67] Hence, a combination of both extraction and purification of the samples is a requirement for a reliable analysis.[68] Various methods, including reversed-phase, size-exclusion, and ion-exchange chromatography as well as solid-phase extraction (SPE), have been employed to isolate and concentrate siderophores.[69−71] However, these approaches often yield inconsistent and suboptimal chromatographic recoveries for siderophores. Additionally, concentrated siderophore fractions obtained by using these methods frequently contain numerous other compounds with similar polarities. To overcome the drawbacks associated with siderophore purification, liquid chromatography methodologies associated with mass spectrometry techniques were later employed in an attempt to facilitate the purification and further identification of siderophores.[69,72−77] However, although these techniques were an improvement over the previous ones, they still present some limitations such as generating false positives due to complex mass signatures or

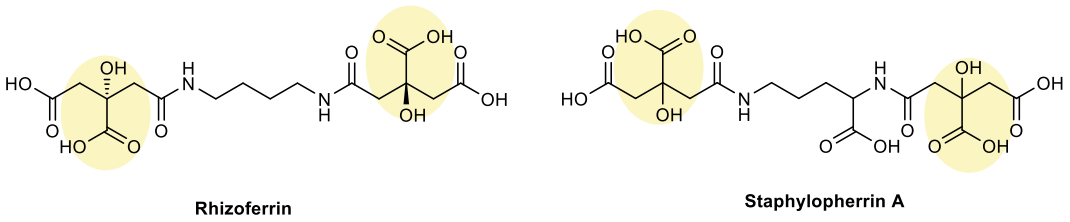

Figure 7. Representative structures of carboxylate-type siderophores.

https://doi.org/10.1021/acsomega.4c03042
ACS Omega 2024, 9, 26863−26877

reduced intensities and detection thresholds caused by ion suppression from coeluting substances.[68]

Immobilized metal affinity chromatography (IMAC) is a sample separation technique mainly used to purify proteins based on the affinities of some proteins to the immobilized metals.[78] The applicability of this technique was also extended to immobilized metal-ion-affinity capillary electrophoresis and, more recently, to the purification of siderophores. The basis of this technique relies on the immobilization of the metal ion in a support matrix and subsequent sample loading, where the active substances are bound to the immobilized metal and separated from the rest of the sample.[78] Hence, Fe(III)-immobilized IMAC columns can be used for the extraction of siderophores from complex samples.[68,78−81] IMAC has a limited range of methodological applications due to a few drawbacks. One of these is that its best siderophore adsorption (hydroxamate) occurs around pH 9, which necessitates adjusting the spent medium or sample to pH 9 before adsorption.[81] A pH-independent chromatographic method would be beneficial in minimizing processing and reducing changes to the natural ratio of ligands in the sample. Certain ligands have a stronger attraction to the immobilized metal cations (such as iron or nickel) than to the IMAC resin itself, which can cause these cations to be removed from the resin. This can result in either the release of the bound ligand or a reduction in the number of available binding sites. Since IMAC only binds free ligands, samples with a high proportion of bound ligands will need to be subjected to a decomplexation process.[81] This can be accomplished using agents such as EDTA, however, it will result in the removal of these ligands from the sample via chromatography, as they can strip metal cations from IMAC and reduce the number of available binding sites.[81] Based on the fact that Ni(II) has a strong affinity toward hydroxamic acids, Ni(II)-IMAC was used to capture pure hydroxamic acids and hydroxamate-containing siderophores, such as desferrioxamine B, from the supernatant of *Streptomyces pilosus* (ATCC 19797) cultured under Fe(III)-deprived conditions.[80] Although this new application represented an advancement on the purification of hydroxamate-containing siderophores directly from bacterial culture supernatants[80] and was even successfully applied to hydroxamate siderophores such as ferrioxamine and ferrichrome,[82,83] other examples were not as successful. IMAC purification of catechol bacillibactin resulted in the recovery of a fragment containing only one catechol group, whereas the complete siderophore with three catecholate groups was not obtained.[78] It was not possible to detect the mixed-ligand siderophore pyoverdine in the eluates obtained from IMAC,[83] indicating that siderophores with high complex stability constants cannot be retained.

A novel type of affinity chromatography that allows for simultaneous analysis of siderophores irrespective of their polarity and complex stability constant was developed and arose as a valuable tool to overcome the current limitations of this methodology. Previous studies showed that catecholates and hydroxamates adsorb well on TiO_2 surfaces, therefore suggesting metal oxide affinity chromatography (MOAC) utilizing TiO_2 as a potential alternative for metal ligand extraction.[84,85] An advanced methodology was developed to efficiently and specifically enrich hydroxamate-type siderophores from complex polar protic matrices, through TiO_2 nanoparticle (NP)-based SPE.[81] The model siderophore desferrioxamine B was used to test the binding capacity of TiO_2 NPs for siderophore extraction. The results showed that TiO_2 NP SPE had a higher binding capacity compared to the IMAC methods, with similar recovery for 1 mg of TiO_2 and 1 mL of IMAC.[81] Alkaline buffers containing phosphate were found to be effective in achieving a high recovery (77.6 ± 6.2%) of desferrioxamine B extracted from complex bacterial culture supernatants. The TiO_2 NP SPE also proved to be a useful cleanup procedure for processing complex samples containing an unknown mixture of siderophores. Since the TiO_2 NP SPE step removed most contaminants, it enabled the detection of siderophores or hydroxamates directly from liquid chromatography−mass spectrometry (LC−MS) base peak chromatograms.[81] After this proof of concept, where it was confirmed that TiO_2 NP SPE is well-suited to extract and elute hydroxamate siderophores from complex matrices,[81] titanium dioxide affinity chromatography (TDAC) was developed for the selective purification of the three main siderophore classes (i.e., catecholates, α-hydroxycarboxylates, and hydroxamates) and mixed ligands.[68] This new and improved methodology is scalable, can selectively purify siderophores, and was able to remove organic "contaminants" almost completely from a bacterial culture supernatant mix containing all four types of model siderophores with recoveries of up to 82% (Petrobactin).[68] Thus, this methodology simplifies the purification of siderophores and may facilitate the discovery and quantification of siderophores in a variety of natural matrices such as seawater, soil, and medical samples.[68] However, TDAC presents a methodological challenge of achieving the same recovery and selectivity for picomolar concentrations of siderophores in natural samples, since other factors will interfere with its efficiency (e.g., coadsorption, self-assembly, metal contamination, and natural phosphate concentrations); nonetheless, it still presents as a robust method against many chromatographically challenging conditions and will facilitate the study of microbial iron cycling, pathogenicity, and symbiosis.[68]

4. SIDEROPHORE CHARACTERIZATION

The isolated/purified siderophores can be characterized by common spectroscopic and spectrometric techniques. Fourier transform infrared (FTIR) analysis can be used to determine the functional groups present in the analyzed siderophores.[47,54,86] Thermal and pH treatments combined with a comprehensive use of curve-fitting analysis can provide improved band resolution, facilitating functional group identification.[87] Additionally, through FTIR analysis, it is possible to identify the functional groups involved in the interaction of the siderophore with the metal by the absence of specific bands in the spectrum when the metal ion is present, indicating that the respective functional groups are involved in the metal bonding.[88] In the chemical and structural characterization of a siderophore produced by marine *Vibrio harveyi*, FTIR and ^{1}H NMR spectra revealed the hydroxamate nature of the siderophore produced.[89] In another study, ultrahigh-performance Fourier transform ion cyclotron resonance mass spectrometry at 21 T was used to detect and identify metal chelators produced by microbes residing in calcareous soils from Eastern Washington.[74] The technique allowed for fast and confident identification of four major classes of siderophores, namely, ferrioxamines, pseudobactins, enterobactins, and arthrobactins. It was observed that each siderophore likely originates from a unique microbial community member and has distinct chemical characteristics and uptake pathways. This

https://doi.org/10.1021/acsomega.4c03042
ACS Omega 2024, 9, 26863−26877

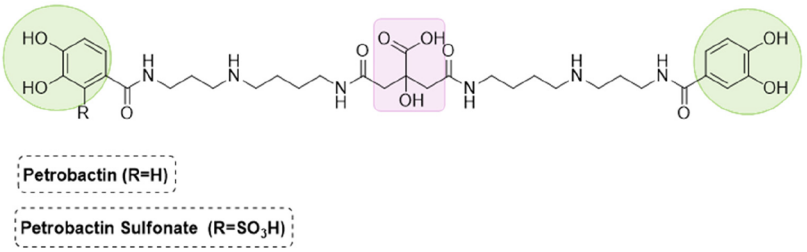

Figure 8. Structure of petrobactin and petrobactin sulfonate.

fierce competition for iron within calcareous soils is likely due to the different siderophore-producing microbes and their specific uptake mechanisms.[74]

NMR spectroscopy is commonly used to identify the structure of siderophores and detect impurities.[54,90−93] For instance, a high similarity of the citrate framework to other citrate-based siderophores such as synechobactins, orchobactin, and acinetobactin was observed in the ^{1}H NMR spectra of chryseochelin A.[94] Additionally, heteronuclear multiple-bond correlation (HMBC) and nuclear Overhauser effect spectroscopy (NOESY) correlations were essential for the structure elucidation of this siderophore.[94] NMR has also been used to study the ability of siderophores to form complexes with different metal ions. In a recent review, attention was devoted to the three natural products derived from *Pseudomonas aeruginosa*, namely, pyocyanin, pyochelin, and pyoverdine(s), and their ability to form complexes with Fe^{2+}, Fe^{3+}, Mn^{2+}, Mn^{3+}, Ga^{3+}, Cr^{3+}, Ni^{2+}, Cu^{2+}, Zn^{2+}, and Cd^{2+}, highlighting the use of NMR for the characterization of the pyochelin−Zn^{2+} and −Ga^{3+} complexes.[95] Other examples include the characterization of the metal complexes of the siderophore desferriferricrocin with Fe^{3+}, Cr^{3+}, Al^{3+}, Ga^{3+}, Cu^{2+}, and Zn^{2+};[96] while the authors were able to obtain the NMR spectra for Al^{3+}, Ga^{3+}, and Zn^{2+}, spectra could not be obtained for Cu^{2+}, Fe^{3+}, and Cr^{3+} due to line broadening from the paramagnetic nature of divalent copper and trivalent iron and chromium.[96]

X-ray diffraction analysis can also be employed in cases where the metal−siderophore complex crystallizes.[23] With this structural analysis, it is possible to reveal the sites where the complexation of the metal occurs.[23]

High-performance liquid chromatography with UV detection (HPLC-UV) analysis is another technique used to characterize siderophores, which puts in evidence any degradation products or the presence of impurities.[47] Through the analysis of the retention times, it is possible to know the polarity of the siderophores due to their affinity for the column. When comparing the aforementioned new petrobactin sulfonate siderophore (Figure 8) with the petrobactin siderophore (Figure 8) in reversed-phase HPLC-MS, it was possible to observe that the most hydrophilic siderophore, i.e., the one with the shortest retention times, is petrobactin sulfonate.[97] In addition, liquid chromatography coupled with tandem mass spectrometry (LC-MS/MS) is a useful technique to identify and characterize siderophores, with their fragments represented by peaks,[90] and has been applied in the identification of siderophores in complex samples, such as soils.[98]

Siderophores have been characterized by mass spectrometry (MS) and associated combinational technologies such as LC−MS, gas chromatography−mass spectrometry (GC−MS), and capillary electrophoresis−mass spectrometry (CE−MS).[99−101] Since the first report of the use of MS to detect enterobactin in 1970,[102] MS has been used to assess various biological molecules in different matrixes over the past 20 years.[103−108] Specifically, several ionization and analytical techniques, such as electrospray-ionization mass spectrometry (ESI-MS), matrix-assisted laser desorption/ionization mass spectrometry (MALDI-MS), inductively coupled plasma mass spectrometry (ICP-MS), and mass spectrometry imaging (MSI), have been used to identify and characterize siderophores.[86,91−93,101,109,110]

External calibration curves are required for some methods to quantify siderophores (e.g.: UV−vis spectrophotometry, fluorescence spectroscopy, HPLC, and MS). In contrast, HPLC−ICP-MS can be used as an alternative method to obtain the necessary data without the need for authentic standards. This methodology offers a response factor independent of the molecular structure of the metal complex and has been suggested for quantifying iron complexes with biological ligands.[111] Another method for the quantification of iron−siderophore complexes without the use of authentic standards has been developed using electrospray high-resolution accurate mass (HRAM) MS.[112] This methodology was applied to peat samples from the French Pyrenean mountains, resulting in the identification and quantification of 19 siderophores belonging to four different classes. The results were then validated using ICP-MS detection of iron by matching the sum of iron complexes determined by isotope exchange−ESI-MS within each peak observed by fast size-exclusion (FastSEC) ICP-MS.[112]

For several years, pyoverdines, siderophores of fluorescent *Pseudomonas*, could usually be differentiated from each other by two physicochemical and physiological methods: siderophore isoelectrofocusing and siderophore-mediated iron uptake.[113,114] In 2008, Meyer[59] introduced mass spectrometry as a useful methodology for the identification of pyoverdines. Thus, mass spectrometry was useful in proving structural differences between compounds not well-differentiated by the two classic siderotyping methods, showing that they can be complementary. The authors advised using them concomitantly for reaching accurate discrimination of pyoverdines and their producing strains through siderotyping.[59] Throughout the years, the structural elucidation and characterization of pyoverdines have required more comprehensive analytical methods because bacterial extracts are complex mixtures. The mass spectrometry techniques evolved and currently allow the rapid identification of this class of siderophores. Rehm et al. developed an approach that uses ultrahigh performance liquid chromatography−ion mobility mass spectrometry (UHPLC−IM-MS) in combination with broadband collision-induced dissociation, which eliminates the need for MS/MS interpretations or specialized equipment for iron uptake or IEF studies. The researchers were able to analyze more than 17 pyoverdines that differ in peptide chain using a timsTOF

https://doi.org/10.1021/acsomega.4c03042
ACS Omega 2024, 9, 26863−26877

Pro.[115] The method utilizes ion mobility spectrometry (IMS) to deliver highly specific collision cross section (CCS) values that can be used to characterize pyoverdines, thus eliminating the need for other analytical methods.[115] The same authors utilized UHPLC−high-resolution tandem mass spectrometry (UHPLC−HR-MS/MS) to separate highly polar pyoverdines and their derivatives.[116] They employed all-ion fragmentation (AIF) to generate mass spectra containing the characteristic fragments of ferribactin, the biological precursor of pyoverdine, allowing the determination of the mass of secreted pyoverdines. The researchers used targeted MS/MS experiments at multiple collisions to accomplish the full structure elucidation of the pyoverdine peptide chain. To facilitate the interpretation of MS/MS spectra, they employed a mass calculator and a fragmentation predictor that provided accurate masses for a straightforward comparison of measured and theoretical values. The method was validated using four well-known pyoverdines with various peptide chains, and it was successfully applied to the analysis of 13 unknown pyoverdines secreted by bacterial cultures. Among these, the researchers discovered four novel pyoverdine peptide chains that were reported for the first time.[116]

Although the determination of the exact mass of a pyoverdine together with its IEF pattern or iron uptake behavior provides sufficient information to unambiguously identify a pyoverdine, this requires the performance of at least two experiments. To avoid that, a comprehensive and easy to replicate universal high-throughput UHPLC−MS/MS pipeline was proposed to elucidate the peptide chain of pyoverdines and their derivatives in bacterial liquid cultures.[117] To avoid the need for iron uptake or IEF experiments, the authors proposed the measurement of CCS values by IMS as an alternative identification marker.[117]

5. GENOMIC APPROACH AND BIOINFORMATIC TOOLS

The increased availability of genome sequences has enabled the development of valuable tools for the prediction and identification of bacterial natural products.[118] Advances in next-generation sequencing technology and analysis over the past 15 years have revolutionized microbial genomics and our ability to unravel a microorganism's metabolic potential through bioinformatic analyses.[119] Since siderophores are assembled by biosynthetic assembly lines involving modular multidomain enzymes such as nonribosomal peptide synthetases (NRPSs), nowadays the purification of these metabolites can be performed through a genome-guided approach, which consists of using the genome sequence in silico for structural and physicochemical prediction to guide the design of the corresponding lab experiments. Genes encoding siderophore biosynthesis, transport, and utilization are generally localized on the genome, forming biosynthetic gene clusters (BGCs).[118] The presence of a putative BGC not only provides evidence that a siderophore is being produced but also can be used to predict the chemical structure of the molecule and dereplicate it against known compounds. Several platforms have been developed for the automated detection of BGCs in a genome, and two of the most popular are antiSMASH and PRISM.[119,120] AntiSMASH is a rapid and reliable source for finding gene clusters responsible for the biosynthesis of secondary metabolites and has been widely applied to the discovery of new and known siderophores.[121−123] The antiSMASH analysis pipeline, designed for bacterial genomes, and its recent counterpart, fungiSMASH for fungal genomes, share a common codebase. Both pipelines offer specific options through their respective web submission forms. PlantiSMASH, a branch of antiSMASH, incorporates plant-specific functionality, including plant-adapted hidden Markov model profiles and cluster detection logic, and supports coexpression analysis.[120] An interesting study reported the genome-guided purification of high amounts of the siderophore ornibactin and the detection of potentially novel burkholdine derivatives produced by *Burkholderia catarinensis* 89T.[124] In that study, the authors, by using genome-guided purification protocols followed by mass spectrometry techniques, were able to detect masses related to putative new derivatives of the siderophore ornibactin and the antifungal burkholdine as well as homoserine lactones probably related to their regulation.[124] The antiSMASH technology was used for the characterization of siderophores from *E. coli* to find the secondary metabolites that cause pathogenicity in urinary tract infections (UTIs).[125] Since UTIs happen when exogenous and endogenous bacteria enter the urinary tract and colonize there, the discovery of secondary metabolites that cause pathogenicity can be used for the development of future pharmaceutical approaches and drugs.[125]

Several useful tools have been developed alongside antiSMASH, including SMURF, which is used for identifying fungal polyketide synthases, NRPSs, and terpenoid gene clusters. Another noteworthy tool is PRISM, which focuses on predicting the chemical structures of biosynthetic pathways. PRISM is linked to the "Genomes-to-Natural Products" platform (GNP), which matches these predictions with MS/MS data, as well as the GRAPE/GARLIC tools, which match such predictions to chemical databases.[120] A recent study explored the newly isolated *Streptomyces thinghirensis* strain HM3 for possible new secondary metabolites to find novel natural products.[126] The in silico analysis by the antiSMASH and PRISM 4 online software for SM-BGCs predicted 16 clusters, including four terpene, one lantipeptide, one siderophore, two polyketide synthase, two NRPS cluster/NRPS-like fragments, two ribosomally synthesized and post-translationally modified peptide products, two butyrolactones, one tRNA-dependent cyclodipeptide synthase, and one other BGC.[126] This study highlighted that *S. thinghirensis* strain HM3 presents a potential new source of secondary metabolites and the usefulness of these genomic approaches.[126]

6. EVALUATION OF COMPLEX DYNAMICS

After the detection and characterization of siderophores, it is essential to perform assays that validate the formation of metal−siderophore complexes. When working with these particular types of chelators, it is essential to consider additional aspects, and this section is projected to give some insights into complexation studies of siderophores.

6.1. Complexation Capacity Assays. Complexation studies are important to evaluate the potential of siderophores to chelate metal ions, testing their efficacy as chelators of different microbial ligands. These assays are performed in various fields of research, including environmental research, when the formation of the metal−siderophore complex is important. The capacity to form stable complexes with the various heavy metals may differ from siderophore to siderophore, since the chelating action depends on several factors, such as pH, geometric conformation, and the presence of other siderophores.[48]

https://doi.org/10.1021/acsomega.4c03042
ACS Omega 2024, 9, 26863−26877

The addition of ferric chloride ($FeCl_3$) in an alkaline solution (pH 9.0) is an example of a procedure used to evaluate the chelating ability of siderophores.[56] The key to determining the complexation ability is the representation of a graph of $[\text{metal ion}]_{solution}/[S]$ versus $[\text{metal ion}]_{added}/[S]$, where [S] stands for the concentration of siderophores determined by the CAS method.[56] Strong complexation is demonstrated when the $[\text{metal ion}]_{added}/[S]$ ratio is increasing and the $[\text{metal ion}]_{solution}/[S]$ ratio remains constant.[56] Atomic absorption spectroscopy with flame atomization (AAS-FA) or inductively coupled plasma optical emission spectrometry (ICP-OES) can be used to determine the concentration of metal ions in solution.[48,56,127] Another methodology widely used to evaluate metal−siderophore complexation involves spectrophotometric assays (e.g., UV−vis and fluorescence spectroscopy). As an example, a solution of $FeCl_3$ and $CdCl_2$ are added to the purified siderophores to form the Fe^{3+}− and Cd^{2+}−siderophore complexes, respectively, and the UV−vis spectra of the metal ions in the absence of siderophores and of the respective metal−siderophore complexes are analyzed.[128] In this assay, the difference in peak intensities highlights the complexation to occur between the siderophore and the metal ions.[128] The formation of the pyoverdine−Mn^{3+} complex was also proved by similar spectrophotometric techniques.[129]

Another relevant advance to identify the existence of metal−siderophore complexes is through the use of potentiometric titrations.[130] In particular, pH titration curves are obtained to highlight the complexation, i.e., a comparative analysis is made between the siderophore pH titration curve and the metal−siderophore complex pH titration curve.[130] These curves are obtained by a graph of pH versus the ratio between the moles of base added and the moles of siderophore present. These pH curves have been used to prove the complexation between a siderophore analog *N*,*N*′-dihydroxy-*N*,*N*′-diisopropylhexanediamide (DPH) and metal ions such as Ca^{2+}, Mg^{2+}, Cu^{2+}, Zn^{2+}, and Mn^{2+}.[130] The pH−potentiometric technique has also been used to determine complexation behavior between hydroxamate and catecholate siderophores and metal ions (Fe^{3+}, Cr^{3+}, Cu^{2+}, Co^{2+}, and Ni^{2+}).[131] Siderophores produced by *Alcaligenes* sp. RZS2 and *P. aeruginosa* RZS3 (hydroxamate- and catecholate-type) have been proven to chelate Mn^{2+}, Ni^{2+}, Zn^{2+}, Cu^{2+}, Co^{2+}, Hg^{2+}, and Ag^{2+} cations using the modified CAS assay.[38] As already explained, CAS agar plates can be prepared with various metals beyond iron, indirectly showing the chelation between siderophores and heavy metals.[38] It is noteworthy that the weak chelation with the mercury and silver metals was demonstrated by the color intensity (less intensity).[38] Uranium complexation with desferrioxamine B (Figure 4) was also confirmed by a modified CAS method.[53] To complete these complexation studies, in silico studies (docking) can also be performed to predict the coordination chemistry and stability of the complex formed. In the case of the previous study, the complexation with uranium was validated by a docking study.[53] In summary, a wide variety of techniques are currently available to prove the binding of the metal to the siderophore, including spectrophotometric assays, potentiometric titrations, modified CAS assays, and docking studies.

7. CONCLUSIONS AND FUTURE PERSPECTIVES

With the growing interest in siderophores and their widespread application in the medical, technological, and environmental fields, it has become essential to establish rapid and reliable analytical methods for their identification and characterization. Accurate and comprehensive information on siderophores is crucial for understanding their potential applications and improving the existing designs as well as for developing new strategies. While many established techniques are available for siderophore analysis, researchers should utilize them in a complementary manner to ensure consistent and accurate results.

Although the traditional detection and identification assays are still quite valid, the innovative modifications performed on these methodologies by complementing them with more instrumental techniques among chromatographic and spectrometric approaches may promise valuable insights into this area in the near future. Current genome mining techniques enable researchers to acquire authentic information and use it for novel applications. The development of in silico methodologies allows a better understanding of the complex dynamics; the identification and suppression of specific genes in pathogenic microorganisms that are responsible for secondary metabolites could be a new gate in providing novel siderophore structures beyond synthetic mimetics. By the use of recombinant DNA technology, siderophore-based molecules can be expressed in recombinant bacteria for agriculture and other industrial processes. Therefore, siderophore research has been escorted by the advances in instrumental and molecular biology techniques made in the last decades, which brought exponential inputs to this field. Structure characterization of siderophores in complex biological matrices continues to be the bottleneck to more significant advances, but “omics” and artificial intelligence can assist in generating novel siderophore structures.

AUTHOR INFORMATION

Corresponding Authors

Emília Sousa − *LQOF - Laboratório de Química Orgânica e Farmacêutica, Departamento de Ciências Químicas, Faculdade de Farmácia, Universidade do Porto, 4050-313 Porto, Portugal; CIIMAR- Centro Interdisciplinar de Investigação Marinha e Ambiental, Terminal de Cruzeiros do Porto de Leixões, 4450-208 Matosinhos, Portugal;* orcid.org/0000-0002-5397-4672; Email: esousa@ff.up.pt

Diana I. S. P. Resende − *LQOF - Laboratório de Química Orgânica e Farmacêutica, Departamento de Ciências Químicas, Faculdade de Farmácia, Universidade do Porto, 4050-313 Porto, Portugal; CIIMAR- Centro Interdisciplinar de Investigação Marinha e Ambiental, Terminal de Cruzeiros do Porto de Leixões, 4450-208 Matosinhos, Portugal; ICBAS - Instituto de Ciências Biomédicas Abel Salazar, Universidade do Porto, 4050-313 Porto, Portugal;* orcid.org/0000-0002-4077-6060; Email: dresende@ff.up.pt

Author

Ana F. R. Gomes − *LQOF - Laboratório de Química Orgânica e Farmacêutica, Departamento de Ciências Químicas, Faculdade de Farmácia, Universidade do Porto, 4050-313 Porto, Portugal; CIIMAR- Centro Interdisciplinar de Investigação Marinha e Ambiental, Terminal de Cruzeiros do Porto de Leixões, 4450-208 Matosinhos, Portugal*

Complete contact information is available at: https://pubs.acs.org/10.1021/acsomega.4c03042

https://doi.org/10.1021/acsomega.4c03042
ACS Omega 2024, 9, 26863−26877

Author Contributions

A.F.R.G.: Investigation and writing the manuscript. E.S.: Conceptualization and reviewing the manuscript. D.I.S.P.R.: Funding, conceptualization, investigation, and reviewing the manuscript.

Notes

The authors declare no competing financial interest.

■ ACKNOWLEDGMENTS

This work was supported by national funds through the Foundation for Science and Technology (FCT) within the scope of Base Funding UIDB/04423/2020 and UIDP/04423/2020 (CIIMAR) and UIDB/04046/2020, by the Norte Portugal Regional Operational Programme (NORTE 2020) under the PORTUGAL 2020 Partnership Agreement, and through the ERDF as a result of Project ATLANTIDA (reference NORTE-01-0145-FEDER-000040). D.I.S.P.R. acknowledges the support from FCT funding under the Scientific Employment Stimulus—Individual Call (ref.2022.00379.CEECIND/CP1728/CT0001, doi:10.54499/2022.00379.CEECIND/CP1728/CT0001).

■ REFERENCES

(1) Kurth, C.; Kage, H.; Nett, M. Siderophores as molecular tools in medical and environmental applications. *Org. Biomol. Chem.* **2016**, *14* (35), 8212−8227.
(2) Gaonkar, T.; Bhosle, S. Effect of metals on a siderophore producing bacterial isolate and its implications on microbial assisted bioremediation of metal contaminated soils. *Chemosphere* **2013**, *93* (9), 1835−1843.
(3) Chen, J.; Guo, Y.; Lu, Y.; Wang, B.; Sun, J.; Zhang, H.; Wang, H. Chemistry and Biology of Siderophores from Marine Microbes. *Mar. Drugs* **2019**, *17* (10), 562.
(4) Southwell, J. W.; Black, C. M.; Duhme-Klair, A.-K. Experimental Methods for Evaluating the Bacterial Uptake of Trojan Horse Antibacterials. *ChemMedChem* **2021**, *16* (7), 1063−1076.
(5) Rayner, B.; Verderosa, A. D.; Ferro, V.; Blaskovich, M. A. T. Siderophore conjugates to combat antibiotic-resistant bacteria. *RSC Med. Chem.* **2023**, *14* (5), 800−822.
(6) Vindeirinho, J. M.; Soares, H. M. V. M.; Soares, E. V. Modulation of Siderophore Production by *Pseudomonas fluorescens* through the Manipulation of the Culture Medium Composition. *Appl. Biochem. Biotechnol.* **2021**, *193* (3), 607−618.
(7) Raines, D. J.; Sanderson, T. J.; Wilde, E. J.; Duhme-Klair, A. K. Siderophores. In *Reference Module in Chemistry, Molecular Sciences and Chemical Engineering*; Elsevier, 2015.
(8) Ahmed, E.; Holmström, S. J. M. Siderophores in environmental research: roles and applications. *Microb. Biotechnol.* **2014**, *7* (3), 196−208.
(9) Fan, D.; Fang, Q. Siderophores for medical applications: Imaging, sensors, and therapeutics. *Int. J. Pharm. (Amsterdam, Neth.)* **2021**, *597*, 120306.
(10) Almeida, M. C.; da Costa, P. M.; Sousa, E.; Resende, D. I. S. P. Emerging Target-Directed Approaches for the Treatment and Diagnosis of Microbial Infections. *J. Med. Chem.* **2023**, *66* (1), 32−70.
(11) Chandrangsu, P.; Rensing, C.; Helmann, J. D. Metal homeostasis and resistance in bacteria. *Nat. Rev. Microbiol.* **2017**, *15* (6), 338−350.
(12) Khasheii, B.; Mahmoodi, P.; Mohammadzadeh, A. Siderophores: Importance in bacterial pathogenesis and applications in medicine and industry. *Microbiol. Res.* **2021**, *250*, 126790.
(13) Negash, K. H.; Norris, J. K. S.; Hodgkinson, J. T. Siderophore-Antibiotic Conjugate Design: New Drugs for Bad Bugs? *Molecules* **2019**, *24* (18), 3314.
(14) Kontoghiorghes, G. J. Advances on Chelation and Chelator Metal Complexes in Medicine. *Int. J. Mol. Sci.* **2020**, *21* (7), 2499.
(15) Kandanapitiye, M. S.; Gott, M. D.; Sharits, A.; Jurisson, S. S.; Woodward, P. M.; Huang, S. D. Incorporation of gallium-68 into the crystal structure of Prussian blue to form $K_{68}Ga_xFe_{1-x}[Fe(CN)_6]$ nanoparticles: toward a novel bimodal PET/MRI imaging agent. *Dalton Trans.* **2016**, *45* (22), 9174−9181.
(16) Pandey, A.; Savino, C.; Ahn, S. H.; Yang, Z.; Van Lanen, S. G.; Boros, E. Theranostic Gallium Siderophore Ciprofloxacin Conjugate with Broad Spectrum Antibiotic Potency. *J. Med. Chem.* **2019**, *62* (21), 9947−9960.
(17) Petrik, M.; Zhai, C.; Haas, H.; Decristoforo, C. Siderophores for molecular imaging applications. *Clin. Transl. Imaging* **2017**, *5* (1), 15−27.
(18) Rapti, S.; Boyatzis, S. C.; Rivers, S.; Pournou, A. Siderophores and their Applications in Wood, Textile, and Paper Conservation. In *Microorganisms in the Deterioration and Preservation of Cultural Heritage*; Joseph, E., Ed.; Springer: Cham, Switzerland, 2021; pp 301−339.
(19) Zytnick, A. M.; Gutenthaler-Tietze, S. M.; Aron, A. T.; Reitz, Z. L.; Phi, M. T.; Good, N. M.; Petras, D.; Daumann, L. J.; Martinez-Gomez, N. C. Discovery and characterization of the first known biological lanthanide chelator. *bioRxiv* **2023**, DOI: 10.1101/2022.01.19.476857.
(20) De Serrano, L. O. Biotechnology of siderophores in high-impact scientific fields. *Biomol. Concepts* **2017**, *8* (3−4), 169−178.
(21) Yin, K.; Wang, Q.; Lv, M.; Chen, L. Microorganism remediation strategies towards heavy metals. *Chem. Eng. J.* **2019**, *360*, 1553−1563.
(22) Hider, R. C.; Kong, X. Chemistry and biology of siderophores. *Nat. Prod. Rep.* **2010**, *27* (5), 637−657.
(23) Neilands, J. B. Methodology of Siderophores. *Struct. Bonding (Berlin)* **1984**, *58*, 1−24.
(24) Payne, S. M. Detection, isolation, and characterization of siderophores. *Methods Enzymol.* **1994**, *235*, 329−344.
(25) Dimkpa, C. Microbial siderophores: Production, detection and application in agriculture and environment. *Endocytobiosis Cell Res.* **2016**, *27* (2), 7−16.
(26) Senthilkumar, M.; Amaresan, N.; Sankaranarayanan, A. Detection of Siderophore Producing Microorganisms. In *Plant-Microbe Interactions: Laboratory Techniques*; Humana: New York, 2021; pp 177−181.
(27) Himpsl, S. D.; Mobley, H. L. T. Siderophore Detection Using Chrome Azurol S and Cross-Feeding Assays. *Methods Mol. Biol.* **2019**, *2021*, 97−108.
(28) Pérez-Miranda, S.; Cabirol, N.; George-Téllez, R.; Zamudio-Rivera, L. S.; Fernández, F. J. O-CAS, a fast and universal method for siderophore detection. *J. Microbiol. Methods* **2007**, *70* (1), 127−131.
(29) Schwyn, B.; Neilands, J. B. Universal chemical assay for the detection and determination of siderophores. *Anal. Biochem.* **1987**, *160* (1), 47−56.
(30) Arora, N. K.; Verma, M. Modified microplate method for rapid and efficient estimation of siderophore produced by bacteria. *3 Biotech* **2017**, *7* (6), 381.
(31) Fekete, F. A.; Chandhoke, V.; Jellison, J. Iron-Binding Compounds Produced by Wood-Decaying Basidiomycetes. *Appl. Environ. Microbiol.* **1989**, *55* (10), 2720−2722.
(32) Milagres, A. M. F.; Machuca, A.; Napoleão, D. Detection of siderophore production from several fungi and bacteria by a modification of chrome azurol S (CAS) agar plate assay. *J. Microbiol. Methods* **1999**, *37* (1), 1−6.
(33) Andrews, M. Y.; Santelli, C. M.; Duckworth, O. W. Layer plate CAS assay for the quantitation of siderophore production and determination of exudation patterns for fungi. *J. Microbiol. Methods* **2016**, *121*, 41−43.
(34) Hu, Q.; Xu, J. A simple double-layered chrome azurol S agar (SD-CASA) plate assay to optimize the production of siderophores by a potential biocontrol agent *Bacillus*. *Afr. J. Microbiol. Res.* **2011**, *5* (25), 4321−4327.
(35) Murakami, C.; Tanaka, A. R.; Sato, Y.; Kimura, Y.; Morimoto, K. Easy detection of siderophore production in diluted growth media

https://doi.org/10.1021/acsomega.4c03042
ACS Omega 2024, 9, 26863−26877

using an improved CAS reagent. *J. Microbiol. Methods* **2021**, *189*, 106310.
(36) Gu, S.; Wan, W.; Shao, Z.; Zhong, W. High-throughput method for detecting siderophore production by rhizosphere bacteria. *Bio-Protoc.* **2021**, *11* (9), e4001.
(37) Sushma, J.; Neeti, K.; Sarrah, R.; Pratibha, S.; Hajra, G. A. S. Optimization of universal Chrome Azurol S (CAS) siderophore detecting media with an economical dye substitute using *Pseudomonas fluorescens* as a test organism. *Res. J. Chem. Environ.* **2021**, *25* (4), 27−34.
(38) Patel, P. R.; Shaikh, S. S.; Sayyed, R. Z. Modified chrome azurol S method for detection and estimation of siderophores having affinity for metal ions other than iron. *Environ. Sustainability* **2018**, *1* (1), 81−87.
(39) Kuzyk, S. B.; Hughes, E.; Yurkov, V. Discovery of Siderophore and Metallophore Production in the Aerobic Anoxygenic Phototrophs. *Microorganisms* **2021**, *9* (5), 959.
(40) Bhattacharya, S.; John, P. J.; Ledwani, L. Microbial siderophores an envisaged tool for asbestos bioremediation - A microcosm approach. *Mater. Today: Proc.* **2021**, *43*, 3110−3116.
(41) Shin, S. H.; Lim, Y.; Lee, S. E.; Yang, N. W.; Rhee, J. H. CAS agar diffusion assay for the measurement of siderophores in biological fluids. *J. Microbiol. Methods* **2001**, *44* (1), 89−95.
(42) Barry, A. L. Procedures for testing antimicrobial agents in agar media: theoretical considerations. In *Antibiotics in Laboratory Medicine*, 2nd ed.; Lorian, V., Ed.; Williams & Wilkins: Baltimore, MD, 1985.
(43) Machuca, A.; Milagres, A. M. F. Use of CAS-agar plate modified to study the effect of different variables on the siderophore production by *Aspergillus*. *Lett. Appl. Microbiol.* **2003**, *36* (3), 177−181.
(44) Le Houedec, S.; Thibault de Chanvalon, A.; Mouret, A.; Metzger, E.; Launeau, P.; Gaudin, P.; Lebeau, T. 2D Image Quantification of Microbial Iron Chelators (Siderophores) Using Diffusive Equilibrium in Thin Films Method. *Anal. Chem.* **2019**, *91* (2), 1399−1407.
(45) Arnow, L. E. Colorimetric Determination of the Components of 3,4-Dihydroxyphenylalaninetyrosine Mixtures. *J. Biol. Chem.* **1937**, *118* (2), 531−537.
(46) Xie, X.; Wang, J.; Yuan, H. High-resolution analysis of catechol-type siderophores using polyamide thin layer chromatography. *J. Microbiol. Methods* **2006**, *67* (2), 390−393.
(47) Nithyapriya, S.; Lalitha, S.; Sayyed, R. Z.; Reddy, M. S.; Dailin, D. J.; El Enshasy, H. A.; Luh Suriani, N.; Herlambang, S. Production, Purification, and Characterization of Bacillibactin Siderophore of *Bacillus subtilis* and Its Application for Improvement in Plant Growth and Oil Content in Sesame. *Sustainability* **2021**, *13* (10), 5394.
(48) Ferreira, C. M. H.; Vilas-Boas, Â.; Sousa, C. A.; Soares, H. M. V. M.; Soares, E. V. Comparison of five bacterial strains producing siderophores with ability to chelate iron under alkaline conditions. *AMB Express* **2019**, *9* (1), 78.
(49) Dave, B. P.; Anshuman, K.; Hajela, P. Siderophores of halophilic archaea and their chemical characterization. *Indian J. Exp. Biol.* **2006**, *44* (4), 340−344.
(50) Stookey, L. L. Ferrozine—a new spectrophotometric reagent for iron. *Anal. Chem.* **1970**, *42* (7), 779−781.
(51) Gillam, A. H.; Lewis, A. G.; Andersen, R. J. Quantitative determination of hydroxamic acids. *Anal. Chem.* **1981**, *53* (6), 841−844.
(52) Paul, A.; Dubey, R. Characterization of Protein Involved in Nitrogen Fixation and Estimation of Co-Factor. *Int. J. Curr. Res. Biosci. Plant Biol.* **2015**, *2*, 89−97.
(53) Rashmi, V.; ShylajaNaciyar, M.; Rajalakshmi, R.; D'Souza, S. F.; Prabaharan, D.; Uma, L. Siderophore mediated uranium sequestration by marine cyanobacterium *Synechococcus elongatus* BDU 130911. *Bioresour. Technol.* **2013**, *130*, 204−210.
(54) Osman, Y.; Gebreil, A.; Mowafy, A. M.; Anan, T. I.; Hamed, S. M. Characterization of *Aspergillus niger* siderophore that mediates bioleaching of rare earth elements from phosphorites. *World J. Microbiol. Biotechnol.* **2019**, *35* (6), 93.
(55) Kotasthane, A. S.; Agrawal, T.; Zaidi, N. W.; Singh, U. S. Identification of siderophore producing and cynogenic fluorescent *Pseudomonas* and a simple confrontation assay to identify potential bio-control agent for collar rot of chickpea. *3 Biotech* **2017**, *7* (2), 137.
(56) Wang, Y.; Huang, W.; Li, Y.; Yu, F.; Penttinen, P. Isolation, characterization, and evaluation of a high-siderophore-yielding bacterium from heavy metal-contaminated soil. *Environ. Sci. Pollution. Res.* **2022**, *29* (3), 3888−3899.
(57) Yoder, M. F.; Kisaalita, W. S. Fluorescence of Pyoverdin in Response to Iron and Other Common Well Water Metals. *J. Environ. Sci. Health, Part A* **2006**, *41* (3), 369−380.
(58) Pawar, M. K.; Tayade, K. C.; Sahoo, S. K.; Mahulikar, P. P.; Kuwar, A. S.; Chaudhari, B. L. Selective ciprofloxacin antibiotic detection by fluorescent siderophore pyoverdin. *Biosens. Bioelectron.* **2016**, *81*, 274−279.
(59) Meyer, J.-M.; Gruffaz, C.; Raharinosy, V.; Bezverbnaya, I.; Schäfer, M.; Budzikiewicz, H. Siderotyping of fluorescent *Pseudomonas*: molecular mass determination by mass spectrometry as a powerful pyoverdine siderotyping method. *BioMetals* **2008**, *21* (3), 259−271.
(60) Holmström, S. J. M.; Lundström, U. S.; Finlay, R. D.; van Hees, P. A. W. Siderophores in forest soil solution. *Biogeochemistry* **2004**, *71* (2), 247−258.
(61) Minnick, A. A.; Eizember, L. E.; McKee, J. A.; Dolence, E. K.; Miller, M. J. Bioassay for siderophore utilization by *Candida albicans*. *Anal. Biochem.* **1991**, *194* (1), 223−229.
(62) Thieken, A.; Winkelmann, G. A novel bioassay for the detection of siderophores containing keto-hydroxy bidentate ligands. *FEMS Microbiol. Lett.* **1993**, *111* (2−3), 281−285.
(63) Manninen, M.; Mattila-Sandholm, T. Methods for the detection of *Pseudomonas* siderophores. *J. Microbiol. Methods* **1994**, *19* (3), 223−234.
(64) Bossier, P.; Verstraete, W. Detection of siderophores in soil by a direct bioassay. *Soil Biol. Biochem.* **1986**, *18* (5), 481−486.
(65) Rabsch, W.; Reissbrodt, R. Investigations of *Salmonella* strains from different clinical-epidemiological origin with phenolate and hydroxamate (aerobactin)-siderophore bioassays. *J. Hyg., Epidemiol., Microbiol., Immunol.* **1988**, *32* (3), 353−360.
(66) Payne, S. M. Detection, isolation, and characterization of siderophores. *Methods Enzymol.* **1994**, *235* (C), 329−344.
(67) Boiteau, R. M.; Mende, D. R.; Hawco, N. J.; McIlvin, M. R.; Fitzsimmons, J. N.; Saito, M. A.; Sedwick, P. N.; DeLong, E. F.; Repeta, D. J. Siderophore-based microbial adaptations to iron scarcity across the eastern Pacific Ocean. *Proc. Natl. Acad. Sci. U. S. A.* **2016**, *113* (50), 14237−14242.
(68) Egbers, P. H.; Zurhelle, C.; Koch, B. P.; Dürwald, A.; Harder, T.; Tebben, J. Selective purification of catecholate, hydroxamate and α-hydroxycarboxylate siderophores with titanium dioxide affinity chromatography. *Sep. Purif. Technol.* **2023**, *307*, 122639.
(69) Zajdowicz, S.; Haller, J. C.; Krafft, A. E.; Hunsucker, S. W.; Mant, C. T.; Duncan, M. W.; Hodges, R. S.; Jones, D. N. M.; Holmes, R. K. Purification and Structural Characterization of Siderophore (Corynebactin) from *Corynebacterium diphtheriae*. *PLoS One* **2012**, *7* (4), No. e34591.
(70) Koppisch, A. T.; Browder, C. C.; Moe, A. L.; Shelley, J. T.; Kinkel, B. A.; Hersman, L. E.; Iyer, S.; Ruggiero, C. E. Petrobactin is the Primary Siderophore Synthesized by *Bacillus anthracis* Str. Sterne under Conditions of Iron Starvation. *Biometals* **2005**, *18* (6), 577−585.
(71) Sayyed, R. Z.; Chincholkar, S. B. Purification of siderophores of *Alcaligenes faecalis* on Amberlite XAD. *Bioresour. Technol.* **2006**, *97* (8), 1026−1029.
(72) Yu, S.; Teng, C.; Liang, J.; Song, T.; Dong, L.; Bai, X.; Jin, Y.; Qu, J. Characterization of siderophore produced by *Pseudomonas syringae* BAF.1 and its inhibitory effects on spore germination and mycelium morphology of *Fusarium oxysporum*. *J. Microbiol.* **2017**, *55* (11), 877−884.

https://doi.org/10.1021/acsomega.4c03042
ACS Omega 2024, 9, 26863−26877

(73) Senthilkumar, M.; Amaresan, N.; Sankaranarayanan, A. Purification of Siderophores by High Performance Liquid Chromatography and Electrospray Ionization-Mass Spectrometry (ESI-MS). In *Plant-Microbe Interactions: Laboratory Techniques*; Humana: New York, 2021; pp 191−192.
(74) Boiteau, R. M.; Fansler, S. J.; Farris, Y.; Shaw, J. B.; Koppenaal, D. W.; Pasa-Tolic, L.; Jansson, J. K. Siderophore profiling of cohabitating soil bacteria by ultra-high resolution mass spectrometry. *Metallomics* **2019**, *11* (1), 166−175.
(75) Boiteau, R. M.; Fitzsimmons, J. N.; Repeta, D. J.; Boyle, E. A. Detection of Iron Ligands in Seawater and Marine Cyanobacteria Cultures by High-Performance Liquid Chromatography-Inductively Coupled Plasma-Mass Spectrometry. *Anal. Chem.* **2013**, *85* (9), 4357−4362.
(76) Baars, O.; Morel, F. M. M.; Perlman, D. H. ChelomEx: Isotope-Assisted Discovery of Metal Chelates in Complex Media Using High-Resolution LC-MS. *Anal. Chem.* **2014**, *86* (22), 11298−11305.
(77) Deicke, M.; Mohr, J. F.; Bellenger, J.-P.; Wichard, T. Metallophore mapping in complex matrices by metal isotope coded profiling of organic ligands. *Analyst* **2014**, *139* (23), 6096−6099.
(78) Li, Y.; Jiang, W.; Gao, R.; Cai, Y.; Guan, Z.; Liao, X. Fe(III)-based immobilized metal-affinity chromatography (IMAC) method for the separation of the catechol siderophore from *Bacillus tequilensis* CD36. *3 Biotech* **2018**, *8* (9), 392.
(79) Simionato, A. V. C.; Silva-Stenico, M. E.; Tsai, S. M.; Carrilho, E. Evidences of siderophores synthesis by Grapevine *Xylella fastidiosa*, causal agent of Pierce's disease, through instrumental approaches. *J. Braz. Chem. Soc.* **2010**, *21* (4), 635−641.
(80) Braich, N.; Codd, R. Immobilised metal affinity chromatography for the capture of hydroxamate-containing siderophores and other Fe(III)-binding metabolites directly from bacterial culture supernatants. *Analyst* **2008**, *133* (7), 877−880.
(81) Egbers, P. H.; Harder, T.; Koch, B. P.; Tebben, J. Siderophore purification with titanium dioxide nanoparticle solid phase extraction. *Analyst* **2020**, *145* (22), 7303−7311.
(82) Ejje, N.; Soe, C. Z.; Gu, J.; Codd, R. The variable hydroxamic acid siderophore metabolome of the marine actinomycete *Salinispora tropica* CNB-440. *Metallomics* **2013**, *5* (11), 1519−1528.
(83) Heine, T.; Mehnert, M.; Schwabe, R.; Tischler, D. Siderophore Purification via Immobilized Metal Affinity Chromatography. *Solid State Phenom.* **2017**, *262*, 505−508.
(84) Upritchard, H. G.; Yang, J.; Bremer, P. J.; Lamont, I. L.; McQuillan, A. J. Adsorption to Metal Oxides of the *Pseudomonas aeruginosa* Siderophore Pyoverdine and Implications for Bacterial Biofilm Formation on Metals. *Langmuir* **2007**, *23* (13), 7189−7195.
(85) Upritchard, H. G.; Yang, J.; Bremer, P. J.; Lamont, I. L.; McQuillan, A. J. Adsorption of Enterobactin to Metal Oxides and the Role of Siderophores in Bacterial Adhesion to Metals. *Langmuir* **2011**, *27* (17), 10587−10596.
(86) Tank, N.; Rajendran, N.; Patel, B.; Saraf, M. Evaluation and biochemical characterization of a distinctive pyoverdin from a *Pseudomonas* isolated from chickpea rhizosphere. *Braz. J. Microbiol.* **2012**, *43* (2), 639−648.
(87) Siebner-Freibach, H.; Yariv, S.; Lapides, Y.; Hadar, Y.; Chen, Y. Thermo-FTIR Spectroscopic Study of the Siderophore Ferrioxamine B: Spectral Analysis and Stereochemical Implications of Iron Chelation, pH, and Temperature. *J. Agric. Food Chem.* **2005**, *53* (9), 3434−3443.
(88) Meesungnoen, O.; Chantiratikul, P.; Thumanu, K.; Nuengchamnong, N.; Hokura, A.; Nakbanpote, W. Elucidation of crude siderophore extracts from supernatants of *Pseudomonas* sp. ZnCd2003 cultivated in nutrient broth supplemented with Zn, Cd, and Zn plus Cd. *Arch. Microbiol.* **2021**, *203* (6), 2863−2874.
(89) Murugappan, R. M.; Aravinth, A.; Karthikeyan, M. Chemical and structural characterization of hydroxamate siderophore produced by marine *Vibrio harveyi*. *J. Ind. Microbiol. Biotechnol.* **2011**, *38* (2), 265−273.
(90) Schwabe, R.; Dittrich, C.; Kadner, J.; Rudi Senges, C. H.; Bandow, J. E.; Tischler, D.; Schlömann, M.; Levicán, G.; Wiche, O. Secondary metabolites released by the rhizosphere bacteria *Arthrobacter oxydans* and *Kocuria rosea* enhance plant availability and soil-plant transfer of germanium (Ge) and rare earth elements (REEs). *Chemosphere* **2021**, *285*, 131466.
(91) Uranga, C. C.; Arroyo, P.; Duggan, B. M.; Gerwick, W. H.; Edlund, A. Commensal Oral *Rothia mucilaginosa* Produces Enterobactin, a Metal-Chelating Siderophore. *mSystems* **2020**, *5* (2), e00161-20.
(92) Sonnenschein, E. C.; Stierhof, M.; Goralczyk, S.; Vabre, F. M.; Pellissier, L.; Hanssen, K. Ø.; de la Cruz, M.; Díaz, C.; de Witte, P.; Copmans, D.; Andersen, J. H.; Hansen, E.; Kristoffersen, V.; Tormo, J. R.; Ebel, R.; Milne, B. F.; Deng, H.; Gram, L.; Jaspars, M.; Tabudravu, J. N. Pseudochelin A, a siderophore of *Pseudoalteromonas piscicida* S2040. *Tetrahedron* **2017**, *73* (18), 2633−2637.
(93) Hermenau, R.; Ishida, K.; Gama, S.; Hoffmann, B.; Pfeifer-Leeg, M.; Plass, W.; Mohr, J. F.; Wichard, T.; Saluz, H.-P.; Hertweck, C. Gramibactin is a bacterial siderophore with a diazeniumdiolate ligand system. *Nat. Chem. Biol.* **2018**, *14* (9), 841−843.
(94) Rehm, K.; Vollenweider, V.; Gu, S.; Friman, V.-P.; Kümmerli, R.; Wei, Z.; Bigler, L. Chryseochelins—structural characterization of novel citrate-based siderophores produced by plant protecting Chryseobacterium spp. *Metallomics* **2023**, *15* (3), mfad008.
(95) Andrejević, T. P.; Ašanin, D. P.; Pantović, B. V.; Stevanović, N. L.; Marković, V. R.; Djuran, M. I.; Glišić, B. Đ. Metal complexes with valuable biomolecules produced by *Pseudomonas aeruginosa*: a review of the coordination properties of pyocyanin, pyochelin and pyoverdines. *Dalton Trans.* **2023**, *52* (14), 4276−4289.
(96) Zou, G.; Boyer, G. L. Synthesis and properties of different metal complexes of the siderophore desferriferricrocin. *Biometals* **2005**, *18* (1), 63−74.
(97) Hickford, S. J. H.; Küpper, F. C.; Zhang, G.; Carrano, C. J.; Blunt, J. W.; Butler, A. Petrobactin Sulfonate, a New Siderophore Produced by the Marine Bacterium *Marinobacter hydrocarbonoclasticus*. *J. Nat. Prod.* **2004**, *67* (11), 1897−1899.
(98) Rai, V.; Fisher, N.; Duckworth, O. W.; Baars, O. Extraction and Detection of Structurally Diverse Siderophores in Soil. *Front. Microbiol.* **2020**, *11*, 581508.
(99) Singh, S.; Hider, R. C.; Porter, J. B. Separation and identification of desferrioxamine and its iron chelating metabolites by high-performance liquid chromatography and fast atom bombardment mass spectrometry: Choice of complexing agent and application to biological fluids. *Anal. Biochem.* **1990**, *187* (2), 212−219.
(100) McCormack, P.; Worsfold, P. J.; Gledhill, M. Separation and Detection of Siderophores Produced by Marine Bacterioplankton Using High-Performance Liquid Chromatography with Electrospray Ionization Mass Spectrometry. *Anal. Chem.* **2003**, *75* (11), 2647−2652.
(101) Su, Q.; Xu, G.; Guan, T.; Que, Y.; Lu, H. Mass spectrometry-derived systems biology technologies delineate the system's biochemical applications of siderophores. *Mass Spectrom. Rev.* **2018**, *37* (2), 188−201.
(102) Pollack, J. R.; Neilands, J. B. Enterobactin, an iron transport compound from *Salmonella typhimurium*. *Biochem. Biophys. Res. Commun.* **1970**, *38* (5), 989−992.
(103) Nielsen, K. F.; Smedsgaard, J. Fungal metabolite screening: database of 474 mycotoxins and fungal metabolites for dereplication by standardised liquid chromatography-UV-mass spectrometry methodology. *J. Chromatogr. A* **2003**, *1002* (1), 111−136.
(104) Henderson, J. P.; Crowley, J. R.; Pinkner, J. S.; Walker, J. N.; Tsukayama, P.; Stamm, W. E.; Hooton, T. M.; Hultgren, S. J. Quantitative Metabolomics Reveals an Epigenetic Blueprint for Iron Acquisition in Uropathogenic *Escherichia coli*. *PLOS Pathog.* **2009**, *5* (2), No. e1000305.
(105) Lv, H.; Henderson, J. P. Yersinia High Pathogenicity Island Genes Modify the *Escherichia coli* Primary Metabolome Independently of Siderophore Production. *J. Proteome Res.* **2011**, *10* (12), 5547−5554.
(106) Chaturvedi, K. S.; Hung, C. S.; Crowley, J. R.; Stapleton, A. E.; Henderson, J. P. The siderophore yersiniabactin binds copper to

https://doi.org/10.1021/acsomega.4c03042
ACS Omega 2024, 9, 26863−26877

protect pathogens during infection. *Nat. Chem. Biol.* **2012**, *8* (8), 731−736.
(107) Lv, H.; Hung, C. S.; Henderson, J. P. Metabolomic Analysis of Siderophore Cheater Mutants Reveals Metabolic Costs of Expression in Uropathogenic *Escherichia coli*. *J. Proteome Res.* **2014**, *13* (3), 1397−1404.
(108) Yan, L.; Nie, W.; Lv, H. Metabolic phenotyping of the *Yersinia* high-pathogenicity island that regulates central carbon metabolism. *Analyst* **2015**, *140* (10), 3356−3361.
(109) Pluháček, T.; Lemr, K.; Ghosh, D.; Milde, D.; Novák, J.; Havlíček, V. Characterization of microbial siderophores by mass spectrometry. *Mass Spectrom. Rev.* **2016**, *35* (1), 35−47.
(110) Gokarn, K.; Sarangdhar, V.; Pal, R. B. Effect of microbial siderophores on mammalian non-malignant and malignant cell lines. *BMC Complementary Altern. Med.* **2017**, *17* (1), 145.
(111) Bundy, R. M.; Boiteau, R. M.; McLean, C.; Turk-Kubo, K. A.; McIlvin, M. R.; Saito, M. A.; Van Mooy, B. A. S.; Repeta, D. J. Distinct Siderophores Contribute to Iron Cycling in the Mesopelagic at Station ALOHA. *Front. Mar. Sci.* **2018**, *5*, 61.
(112) Maknun, L.; Kińska, K.; González-Álvarez, I.; Ouerdane, L.; Lauga, B.; Siripinyanond, A.; Szpunar, J.; Lobinski, R. Quantitative Determination of Iron-Siderophore Complexes in Peat by Isotope-Exchange Size-Exclusion UPLC-Electrospray Ionization High-Resolution Accurate Mass (HRAM) Mass Spectrometry. *Anal. Chem.* **2023**, *95* (24), 9182−9190.
(113) Schlegel, K.; Fuchs, R.; Schäfer, M.; Taraz, K.; Budzikiewicz, H.; Geoffroy, V.; Meyer, J.-M. The Pyoverdins of *Pseudomonas* sp. 96-312 and 96-318. *Z. Naturforsch. C* **2001**, *56* (9−10), 680−686.
(114) Meyer, J.-M.; Geoffroy, V. A.; Baysse, C.; Cornelis, P.; Barelmann, I.; Taraz, K.; Budzikiewicz, H. Siderophore-Mediated Iron Uptake in Fluorescent *Pseudomonas*: Characterization of the Pyoverdine-Receptor Binding Site of Three Cross-Reacting Pyoverdines. *Arch. Biochem. Biophys.* **2002**, *397* (2), 179−183.
(115) Rehm, K.; Vollenweider, V.; Kümmerli, R.; Bigler, L. Rapid identification of pyoverdines of fluorescent *Pseudomonas* spp. by UHPLC-IM-MS. *BioMetals* **2023**, *36* (1), 19−34.
(116) Rehm, K.; Vollenweider, V.; Kümmerli, R.; Bigler, L. A comprehensive method to elucidate pyoverdines produced by fluorescent *Pseudomonas* spp. by UHPLC-HR-MS/MS. *Anal. Bioanal. Chem.* **2022**, *414* (8), 2671−2685.
(117) Rehm, K.; Vollenweider, V.; Kümmerli, R.; Bigler, L. Pyoverdine Analysis—From High-Resolution MS/MS Fragmentation to Ion Mobility Measurements. *Chimia* **2023**, *77* (4), 250−253.
(118) Terra, L.; Ratcliffe, N.; Castro, C. H.; Vicente, C. P. A.; Dyson, P. Biotechnological Potential of *Streptomyces* Siderophores as New Antibiotics. *Curr. Med. Chem.* **2021**, *28* (7), 1407−1421.
(119) Reitz, Z. L.; Medema, M. H. Genome mining strategies for metallophore discovery. *Curr. Opin. Biotechnol.* **2022**, *77*, 102757.
(120) Blin, K.; Kim, H. U.; Medema, M. H.; Weber, T. Recent development of antiSMASH and other computational approaches to mine secondary metabolite biosynthetic gene clusters. *Briefings Bioinf.* **2019**, *20* (4), 1103−1113.
(121) Calderón Celis, F.; González-Álvarez, I.; Fabjanowicz, M.; Godin, S.; Ouerdane, L.; Lauga, B.; Łobiński, R. Unveiling the Pool of Metallophores in Native Environments and Correlation with Their Potential Producers. *Environ. Sci. Technol.* **2023**, *57* (45), 17302−17311.
(122) Toymentseva, A. A.; Pudova, D. S.; Sharipova, M. R. Identification of Secondary Metabolite Gene Clusters in the Genome of *Bacillus pumilus* Strains 7P and 3−19. *BioNanoScience* **2019**, *9* (2), 313−316.
(123) Gosse, J. T.; Ghosh, S.; Sproule, A.; Overy, D.; Cheeptham, N.; Boddy, C. N. Whole Genome Sequencing and Metabolomic Study of Cave *Streptomyces* Isolates ICC1 and ICC4. *Front. Microbiol.* **2019**, *10*, 1020.
(124) Bach, E.; Chen, J.; Angolini, C. F. F.; Bauer, J. S.; Gross, H.; Passaglia, L. M. P. Genome-guided purification of high amounts of the siderophore ornibactin and detection of potentially novel burkholdine derivatives produced by *Burkholderia catarinensis* 89T. *J. Appl. Microbiol.* **2024**, *135* (2), lxae040.
(125) Cavas, L.; Kirkiz, I. Characterization of siderophores from *Escherichia coli* strains through genome mining tools: an antiSMASH study. *AMB Express* **2022**, *12* (1), 74.
(126) Rehan, M.; Gueddou, A.; Alharbi, A.; Ben Abdelmalek, I. In Silico Prediction of Secondary Metabolites and Biosynthetic Gene Clusters Analysis of *Streptomyces thinghirensis* HM3 Isolated from Arid Soil. *Fermentation* **2023**, *9* (1), 65.
(127) Villén, M.; Lucena, J. J.; Cartagena, M. C.; Bravo, R.; García-Mina, J.; de la Hinojosa, M. I. M. Comparison of Two Analytical Methods for the Evaluation of the Complexed Metal in Fertilizers and the Complexing Capacity of Complexing Agents. *J. Agric. Food Chem.* **2007**, *55* (14), 5746−5753.
(128) Singh, A.; Kaushik, M. S.; Srivastava, M.; Tiwari, D. N.; Mishra, A. K. Siderophore mediated attenuation of cadmium toxicity by paddy field cyanobacterium *Anabaena oryzae*. *Algal Res.* **2016**, *16*, 63−68.
(129) Parker, D. L.; Morita, T.; Mozafarzadeh, M. L.; Verity, R.; McCarthy, J. K.; Tebo, B. M. Inter-relationships of MnO_2 precipitation, siderophore-Mn(III) complex formation, siderophore degradation, and iron limitation in Mn(II)-oxidizing bacterial cultures. *Geochim. Cosmochim. Acta* **2007**, *71* (23), 5672−5683.
(130) Martins, J. G.; Ferreira, C. M. H.; Dey, S. S.; Barros, M. T.; Soares, H. M. V. M. *N*,*N*′-Dihydroxy-*N*,*N*′-diisopropylhexanediamide, a siderophore analogue, as a possible iron chelating agent for hydroponic conditions: metal equilibrium studies. *J. Iran. Chem. Soc.* **2017**, *14* (5), 1079−1088.
(131) Fazary, A. E.; Al-Shihri, A. S.; Saleh, K. A.; Alfaifi, M. Y.; Alshehri, M. A.; Elbehairi, S. E. I. Di- and Tri-valent Metal Ions Interactions with Four Biodegradable Hydroxamate and Cataecholate Siderophores: New Insights into Their Complexation Equilibria. *J. Solution Chem.* **2016**, *45* (5), 732−749.

https://doi.org/10.1021/acsomega.4c03042
ACS Omega 2024, 9, 26863−26877